
Application of Independent Component Analysis in GRACE-Derived Water Storage Changes Interpretation: A Case Study of the Tibetan Plateau and Its Surrounding Areas

Hanjiang Wen, Zhenwei Huang, Youlei Wang, Huanling Liu, and Guangbin Zhu

Abstract

Independent component analysis (ICA) is applied to decompose the water storage changes derived from 132 months (2003.01 to 2013.12) Gravity Recovery and Climate Experiment (GRACE) measurements over Tibetan Plateau. The results are then compared with those from NOAA and WaterGAP Global Hydrology Model (WGHM) hydrological models. Our assessments indicate that the decomposed components from the water storage changes and hydrological models agree well, indicating the ICA's relatively robust performance in separating independent pattern from water storage observations with few a priori information.

Keywords

GRACE • Hydrological Models • Independent Component Analysis • Water Storage Changes

1 Introduction

Extracting information about the large-scale water storage change is very useful to improve the efficiency of water resources development and to understand the water cycle. Gravity Recovery and Climate Experiment (GRACE) gravity mission provides gravity field products, which can be used to monitor the worldwide terrestrial water storage changes (Tapley et al. 2004). However, GRACE measures total gravity changes, which are mainly caused by storage changes in various storage compartments such as the terrestrial water

storage changes, surface water, and groundwater compartments. Therefore, signal separation techniques are required to enhance a better understanding the source of variability derived from GRACE products (Forootan et al. 2014).

Several methods exist that can be used to extract specific patterns from multi-dimensional data are currently used, most of which try to represent a large portion of the variance in the data to reduce the dimension. Among these methods, Empirical Orthogonal Function (EOF, also known as Principal Component Analysis) and its extension methods such as rotated EOF (REOF) and MSSA have made a wide range of applications (Jeffers 1967; Niu et al. 2002; Price et al. 2006; Rangelova et al. 2007; Schrama et al. 2007; Zotov and Shum 2010).

In the decomposition process, the methods mentioned above only use the empirical covariance matrix or correlation matrix of the data sets, that contains only up to second order statistical information, while ignoring the higher-order statistical information. In general, when the probability distribution function of the observations follows a Gaussian distribution, nearly no information is available in higher-order statistical moments (Hyvarinen 1999). When the distribution function follows a non-Gaussian distribution, using

H. Wen • Z. Huang (✉) • Y. Wang
Chinese Academy of Surveying and Mapping, Beijing 100830, China
e-mail: huangzw@casm.ac.cn

H. Liu
Chinese Academy of Surveying and Mapping, Beijing 100830, China
School of Geodesy and Geomatics, Wuhan University, Wuhan 430079, China

G. Zhu
Satellite Surveying and Mapping Application Center, NASG, Beijing 101300, China

the covariance only might not be enough to measure the statistical relationships between different samples (e.g., storage observations). However, one can see that the probability distribution function of GRACE-derived water storage time series is often non-Gaussian (Forootan and Kusche 2012). Further, with uncorrelated and orthogonal hypothesis, the EOF analysis provides the signal components which might not be necessarily interpretable (Jolliffe 2003).

To incorporate more statistical information from the probability distribution function, Cardoso (1992) proposed to add higher-order statistical moments to the EOF method, which is the origin of the Independent Component Analysis (ICA) method. ICA is originally developed for solving blind source separation problems with no or little priori information about the source signals. It has been widely applied in the biomedical field, face recognition, mobile phone communications and other fields (Makeig et al. 1996; Hyvärinen et al. 2004; Bartlett 2001). In recent years, ICA has also been applied in the separation of seismic data, processing of GPS multipath error and GRACE satellite data (Lv et al. 2007; Luo et al. 2012; Guo et al. 2014; Frappart et al. 2010; Forootan and Kusche 2012, 2013; Boergens et al. 2014). In this paper, we follow the approach in Forootan and Kusche (2012).

In this paper, we will first illustrate the data that was used in this study. Then the ICA method that will be used to separate water cycle signals from GRACE-derived water storage changes for better interpretation of detected anomalies over the Tibetan Plateau and its surrounding areas (20° to 40° N, 70° to 100° E) was introduced. To verify the reliability of the results, we decompose and compare the components deriving from the GRACE-derived water storage changes and hydrological models in the same region respectively. Finally, conclusions are summarized based on the comparison results.

2 Data

2.1 GRACE Gravity Field Products

Launched in March 2002, the GRACE mission is the first gravity satellites that can be studied directly for the Earth surface mass changes. The mission determines the variations of the Earth's gravity field which can be used to acquire the land water storage changes after removing other effects, including glacial isostatic adjustment process, mass changes within the ocean and atmosphere etc. Many studies have been done in these aspects, such as the detection to the mass changes of the Antarctic and to study global water storage changes from GRACE monthly gravity field models (Chen et al. 2006; Zhu et al. 2008).

In this paper, we used 132 months spherical harmonic gravity field models from January 2003 to December 2013 provided by Center for Space Research (CSR). The spherical

harmonic coefficients of the GRACE RL05 data were computed to degree and order 60, the effects of tidal, atmosphere and oceans have been deducted in the calculation process. The gravity field variations of GRACE primarily reflect the water storage changes in land areas. The term C_{20} was replaced by the Satellite Laser Ranging observation. The GRACE-derived land water storage changes were obtained after accounting for the glacial isostatic adjustment, decorrelation and Gaussian filter (with 350 km radius) (Chen et al. 2005; Duan et al. 2009; Wen et al. 2011). The results are prepared in $1^\circ \times 1^\circ$ grid.

2.2 Hydrological Models

NASA Goddard Earth Sciences Data and Information Services Center and the National Centers for Environmental Prediction jointly established the Global Land Data Assimilation System (GLDAS) which uses the latest ground modeling and space observation systems to provide parameters of the topography model data (Rodell et al. 2004). Based on NOAA land surface model, GLDAS hydrological model utilized rainfall and solar radiation observations as input parameters to calculate terrestrial water storage changes. It can also be used for verification of GRACE-derived water storage changes information. In this paper, the spatial resolution of the NOAA is the same as GRACE-derived water storage changes, and data is from January 2003 to December 2013, unfortunately the groundwater compartment is not included in the GLDAS.

WaterGAP Global Hydrology Model (WGHM) uses a conceptual framework to simulate continental water cycle. The model was originally developed in the study of continental water resources availability by Döll et al. (2003). Because the model provides the estimation of water mass change, which makes it useful to global water reserves and its dynamic hydrological analysis (Werth and Güntner 2010), WGHM hydrological model has been repeatedly used to compare changes in land water storage and GRACE-derived water storage (Schmidt et al. 2008). The WGHM model in the article uses the same spatial resolution as GRACE-derived water storage changes, from January 2003 to April 2012 that is available to us (personal communication).

3 ICA Method

If the equivalent water height (EWH) at m grid points are derived from n monthly gravity field models, the grids are arranged from north to south with longitudes and latitudes varying as. This time series of observations can be written as a matrix \mathbf{X} , as

$$\mathbf{X} = [\mathbf{x}_1, \mathbf{x}_2, \dots, \mathbf{x}_m] \quad (1)$$

where \mathbf{x}_i is the i -th column, represents the equivalent water height of i -th grid points at different months, i.e. $\mathbf{x}_i = [x_{1i}, \dots, x_{ni}]^T, i = 1, \dots, m$. The EOF decomposition of \mathbf{X} can be expressed as

$$\mathbf{X} = \mathbf{P}\mathbf{E}^T \quad (2)$$

where \mathbf{P} contains the principal components, \mathbf{E} contains the eigenvectors of \mathbf{X} that are normalized to unit vectors in the processing. The important characteristics of time series are contained in the eigenvalues and eigenvectors. Then, we sorted the eigenvectors in order according to corresponding magnitude of eigenvalues.

Independent Component Analysis (ICA) is a method searching for its intrinsic factor or component from multidimensional statistics. The main purpose of ICA is to make the principal components or eigenvectors as independent as possible. The ICA decomposition can be written as follows

$$\mathbf{X} = (\mathbf{P}\mathbf{R}) (\mathbf{R}^T \mathbf{E}^T) = \mathbf{S}\mathbf{A}^T \quad (3)$$

Where \mathbf{A} is called the mixing matrix, \mathbf{S} is the source signal matrix and \mathbf{R} is an orthogonal rotation matrix ($\mathbf{R}\mathbf{R}^T = \mathbf{I}$).

Suppose observations are composed of some unknown non-Gaussian distribution signals \mathbf{S} , then the ICA method can separate independent sources from these mixed observations. Rotation matrix \mathbf{R} is calculated from Joint Approximate Diagonalization of Eigenmatrixes (JADE) method proposed by Cardoso and Souloumiac (1993).

If the mean of column vector $\mathbf{z}_i, \mathbf{z}_j, \mathbf{z}_k, \mathbf{z}_l$ ($1 \leq i, j, k, l \leq n$) are zero, its fourth-order cumulant is defined as

$$\begin{aligned} Cum(\mathbf{z}_i, \mathbf{z}_j, \mathbf{z}_k, \mathbf{z}_l) &= E(\mathbf{z}_i \mathbf{z}_j \mathbf{z}_k \mathbf{z}_l) - E(\mathbf{z}_i \mathbf{z}_j) E(\mathbf{z}_k \mathbf{z}_l) \\ &\quad - E(\mathbf{z}_i \mathbf{z}_k) E(\mathbf{z}_j \mathbf{z}_l) - E(\mathbf{z}_i \mathbf{z}_l) E(\mathbf{z}_j \mathbf{z}_k) \end{aligned} \quad (4)$$

For any $n \times n$ order matrix \mathbf{M} , we can define a $n \times n$ fourth-order cumulant matrix $\mathbf{Q}(\mathbf{M})$ whose (i, j) element is given as

$$[\mathbf{Q}(\mathbf{M})]_{ij} = \sum_{k=1}^n \sum_{l=1}^n Cum(\mathbf{z}_i, \mathbf{z}_j, \mathbf{z}_k, \mathbf{z}_l) \mathbf{m}_{kl} \quad (5)$$

where m_{kl} is the (k, l) elements of \mathbf{M} . Because \mathbf{Z} is centralized, we can get

$$\begin{aligned} \mathbf{Q}(\mathbf{M}) &= E\{(\mathbf{Z}^T \mathbf{M} \mathbf{Z})(\mathbf{Z} \mathbf{Z}^T)\} - \mathbf{C}_Z \text{tr}(\mathbf{M} \mathbf{C}_Z) \\ &\quad - \mathbf{C}_Z \mathbf{M} \mathbf{C}_Z - \mathbf{C}_Z \mathbf{M}^T \mathbf{C}_Z \end{aligned} \quad (6)$$

where \mathbf{C}_Z is the covariance matrix of \mathbf{Z} , tr is the trace of a matrix. Then we can find a normalized orthogonal matrix \mathbf{R} that is joint diagonalization for all fourth-order cumulant matrixes to make $\mathbf{Q}(\mathbf{M})$ diagonalized as possible (Cardoso 1999).

After the EOF decomposition, we can estimate the cumulant matrix $\mathbf{Q}(\mathbf{M})$ of \mathbf{P} or \mathbf{E} from Eq. (6), written as

$$F(\mathbf{R}) = \sum_{m=1}^{n^2} f(\mathbf{R}^T \mathbf{Q}(\mathbf{M}_m) \mathbf{R}) \quad (7)$$

where function f represents the quadratic sum of the non-diagonal elements of matrix. The cumulant matrix $\mathbf{Q}(\mathbf{M})$ is optimized through the plane of rotation under the constraints of \mathbf{R} , when squares of non-diagonal elements in (7) is the least, \mathbf{R} is the optimal solution. Finally, the rotated independent components or spatial patterns are calculated, the corresponding principal components or spatial patterns are acquired from data projector (Frootan and Kusche 2012).

In this study, the temporal ICA method is used. It needs two steps to decompose the water storage changes by using temporal ICA method. First, EOF is conducted to decompose the water storage changes to obtain the dominant orthogonal modes in descending order. Second, the principal components are rotated temporally as mutually independent as possible by the rotation matrix \mathbf{R} that determined by the relevant criterion based on Eq. (5). Then the spatial patterns are determined by rotating the corresponding spatial patterns.

4 Results

4.1 GRACE-Derived Water Storage Changes

We first analyze GRACE-derived water storage changes in Tibetan Plateau and its surrounding areas. The kurtosis of the time series is calculated as $E(X^4)/E(X^2)^2 - 3$ (where E is the expectation operator). Results show that 62.7% of the absolute kurtosis value is greater than 0.5, which means that it is a non-Gaussian distribution.

The auto-covariance matrix of the sample is calculated from the centralized data, and it is diagonalized by eigenvalue decomposition method. The first eigenvalue takes 75.9% of the total energy, which is much larger than the other eigenvalues. The second, third and fourth eigenvalue takes 10.0%, 7.8% and 2.1% of the total energy respectively. The corresponding components of the first four eigenvalues contain about 95.8% of the total energy, so the other components are assumed to be insignificant.

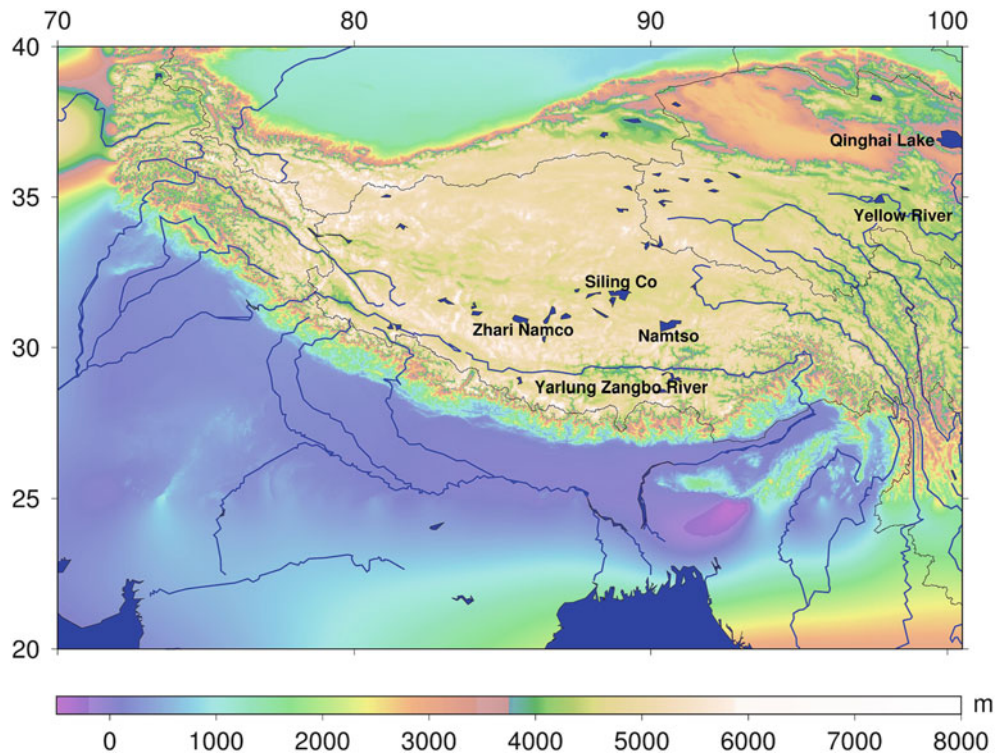


Fig. 1 The major rivers and lakes (*Blue*) over Tibetan Plateau and its surrounding areas

4.2 The Results of ICA Method

Assuming that signals from the GRACE-derived water storage changes are as independent as possible, we use temporal ICA method to analyze the GRACE-derived water storage changes in Tibetan Plateau and its surrounding areas. Figure 1 presents the map of Tibetan Plateau and its surrounding areas. The result of GRACE-derived water storage changes by ICA method in the Tibetan Plateau region was shown in Fig. 2. The temporal components were scaled by standard deviation, and the corresponding spatial patterns had also been multiplied by the same standard deviations to have a unit similar TWS fields. Then water storage changes can be reconstructed by multiplying the spatial components with the corresponding temporal components.

From Fig. 2, the first and second components display a strong annual period signal, the third component is a mixed signal of annual period and long-term trend, and the fourth component contains the annual and semi-annual period signal. IC1 (Independent Component 1, the same below) and IC2 that represents annual periodic signals are more obvious in the southern region, and periodic signals relatively weak in the northern region, which can be interpreted as the annual variation in precipitation. From the long-term trends of IC3, the water reserves of the Tibetan Plateau in western and southern regions reduced in January 2003 to December 2013 period, which is associated with the melting glaciers

and shrinking snowpack. Meanwhile, the water reserves in central region of the Tibetan Plateau have increased that is associated with the increasing area of the plateau lakes. According to Zhang et al. (2013), the mean lake level increased 0.14 m/year for the 200 lakes over Tibetan Plateau and 0.20 m/year for the lakes in the central Tibetan Plateau with 4–7 years satellite altimetry observations, which might be associated with the increasing rainfall, melting snow, and the reducing evaporation of the region in recent years (Zhang et al. 2013).

5 Comparison with the Hydrological Models

Water storage changes from hydrological models represent significant non-Gaussian characteristics, because the existence of the complicated hydrological process, the hydrological data and model structure errors. The rate of absolute kurtosis value (greater than 0.5) calculated using NOAH or WGHM time series is about 68.7% and 71.4%, so showing that the outcomes of hydrological models are also of non-Gaussian distribution. Figure 3 shows that the RMSs of the GRACE-derived water storage changes, NOAH and WGHM hydrological models. The red curve is the 12-points weighted moving average results in order to remove the effects of seasonal variations. From Fig. 3, the water storage changes

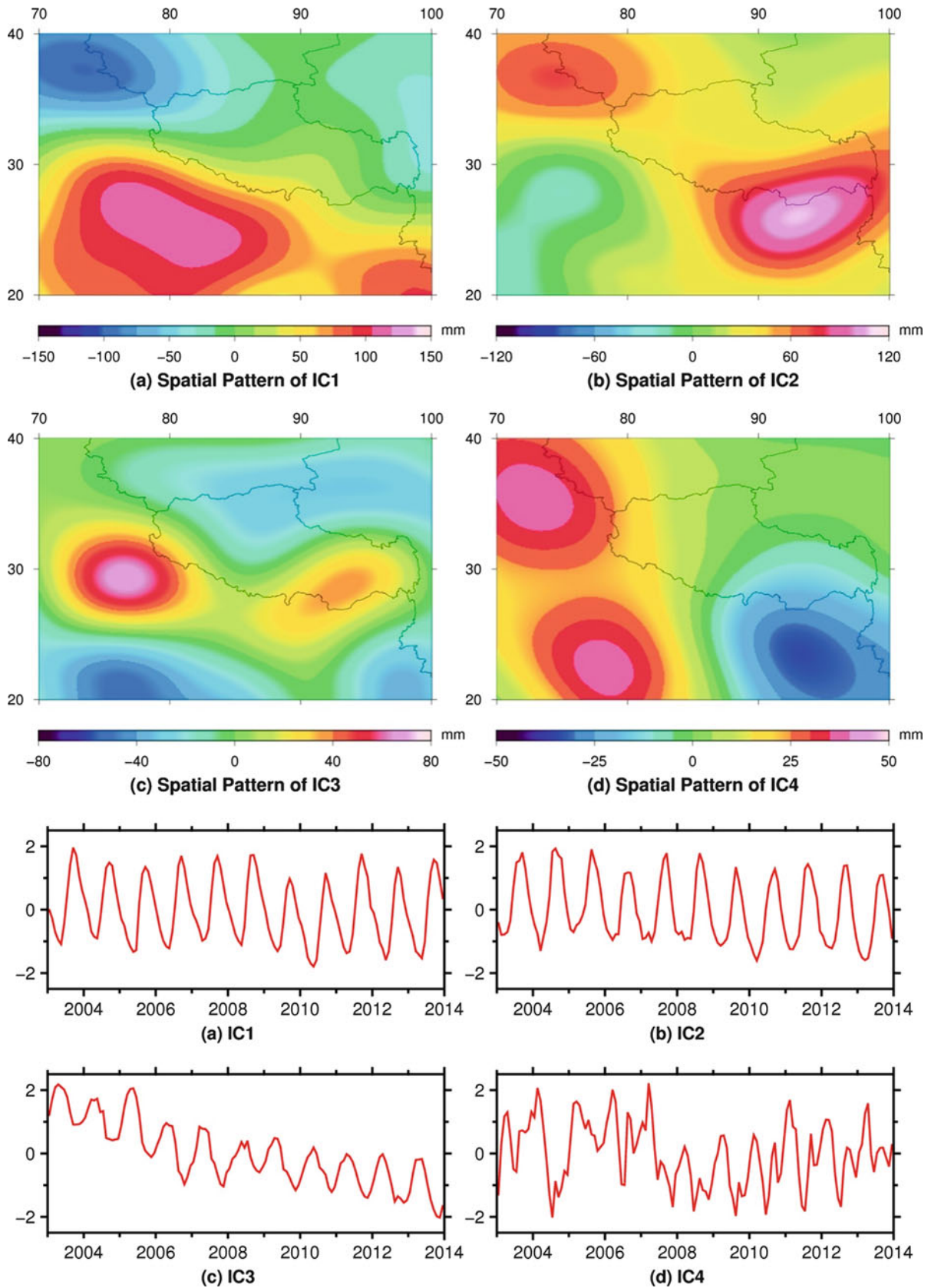


Fig. 2 Spatial pattern (*up*) and time series (*down*) by ICA analysis using 132 months GRACE-derived water storage changes

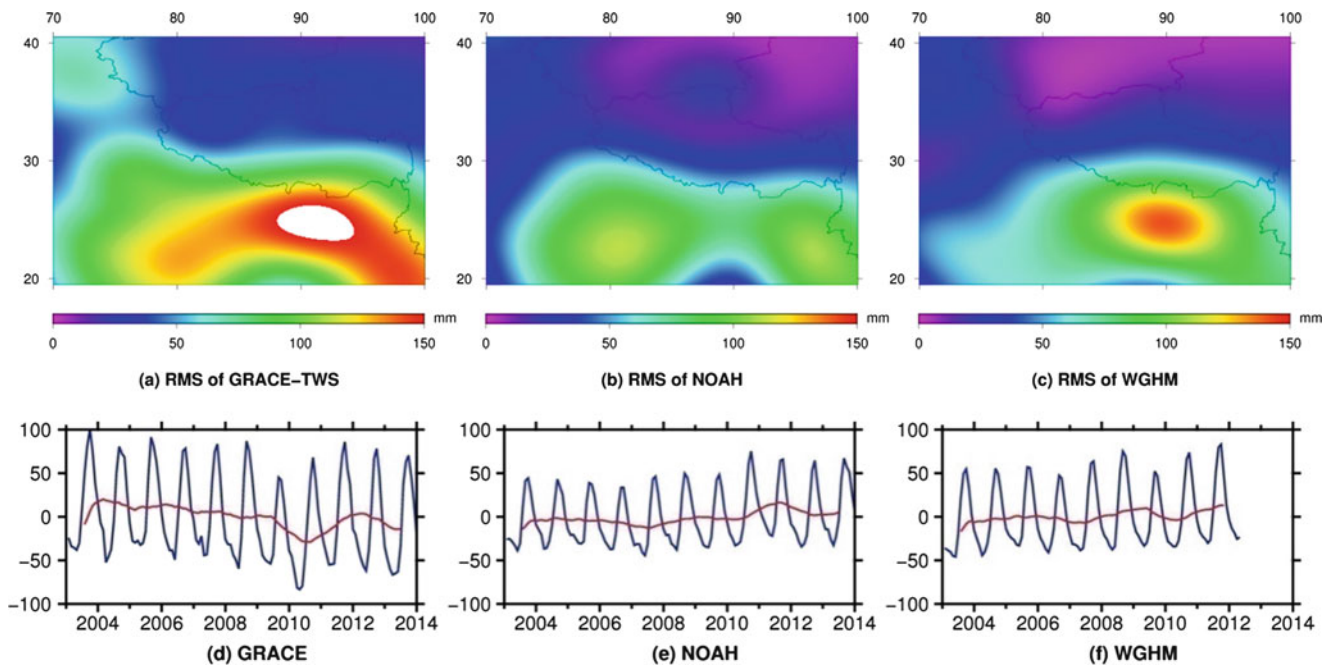


Fig. 3 Signal strength (*up*) and time series (*down*) of GRACE-derived water storage changes and hydrological models, red curve is the moving average of the time series

show significant changes in annual periodicity in the region. The period of GRACE-derived water storage changes is very similar with hydrological models, but the signal strength of GRACE-derived water storage changes is larger than the hydrological models, which indicates that GRACE-derived water storage changes may include the groundwater changes and other factors.

5.1 Results of Hydrological Models

The independent patterns of NOAH and WGHM hydrological models extracted by ICA method are shown in Figs. 4 and 5. From Fig. 4, the first, third and the fourth components of NOAH hydrological model exhibit significant annual period, and the third component contains a long-term trend signal, the second component contains mainly semi-annual period signal. In Fig. 5, the four components of WGHM contain obvious annual periodic signal.

5.2 The Comparison Between Results from GRACE and the Hydrological Models

To verify the reliability of the results, time series of the independent components from both GRACE and hydrological models are compared and the results were shown in Fig. 6. The correlation coefficients between the corresponding com-

ponents are calculated and shown in Table 1. As can be seen from Fig. 6, the periodic signal IC1 of GRACE-derived water storage changes and hydrological models results agree well, correlation coefficients between GRACE&NOAH and GRACE&WGHM are 0.884 and 0.877. IC1 is mainly annual periodic signal, but IC3 is mainly the long-term trend signal and some discrepancies exist between GRACE-derived water storage changes and hydrological models, this is likely due to the fact that: (1) the observations of hydrological models in Tibetan Plateau are less, but observations of the GRACE satellite can cover whole region; (2) hydrological models reflect major changes in surface water (including precipitation, snow melt, wetland changes, etc.), but GRACE-derived water storage changes also includes the groundwater changes, ignoring the groundwater changes in hydrology models may lead to some errors; (3) In addition, different models are calculated by different methods, the results will unavoidably introduce some errors which can be seen from the analysis results of NOAH and WGHM hydrological models.

6 Conclusions

In this paper, we studied the water storage changes of the Tibetan Plateau and its surrounding areas in large-scale by ICA method. The independent components results of GRACE-derived water storage changes and hydrological models are found being in good agreement. The correlation

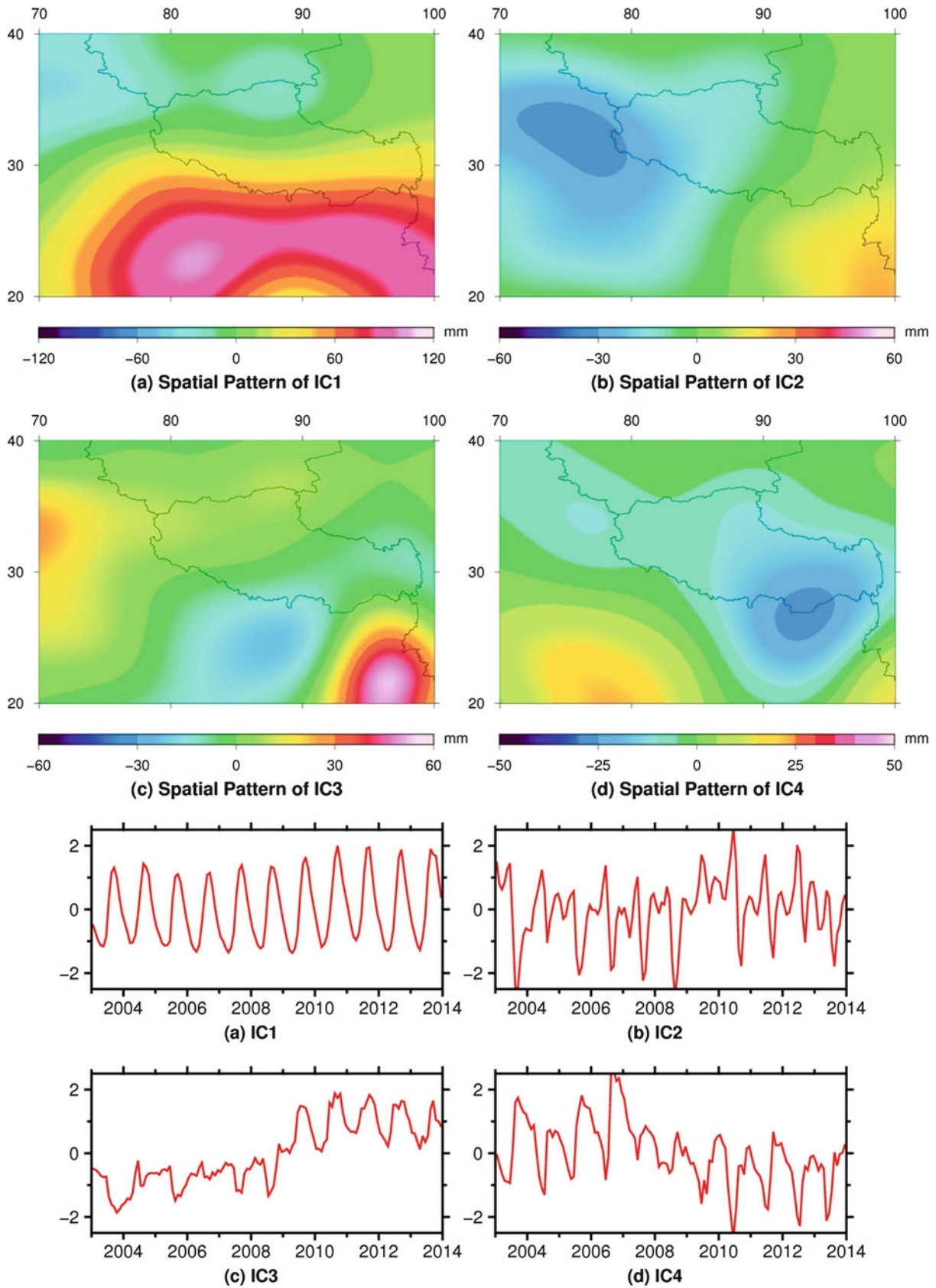


Fig. 4 Spatial pattern (*up*) and time series (*down*) by ICA analysis using 132 months NOAH

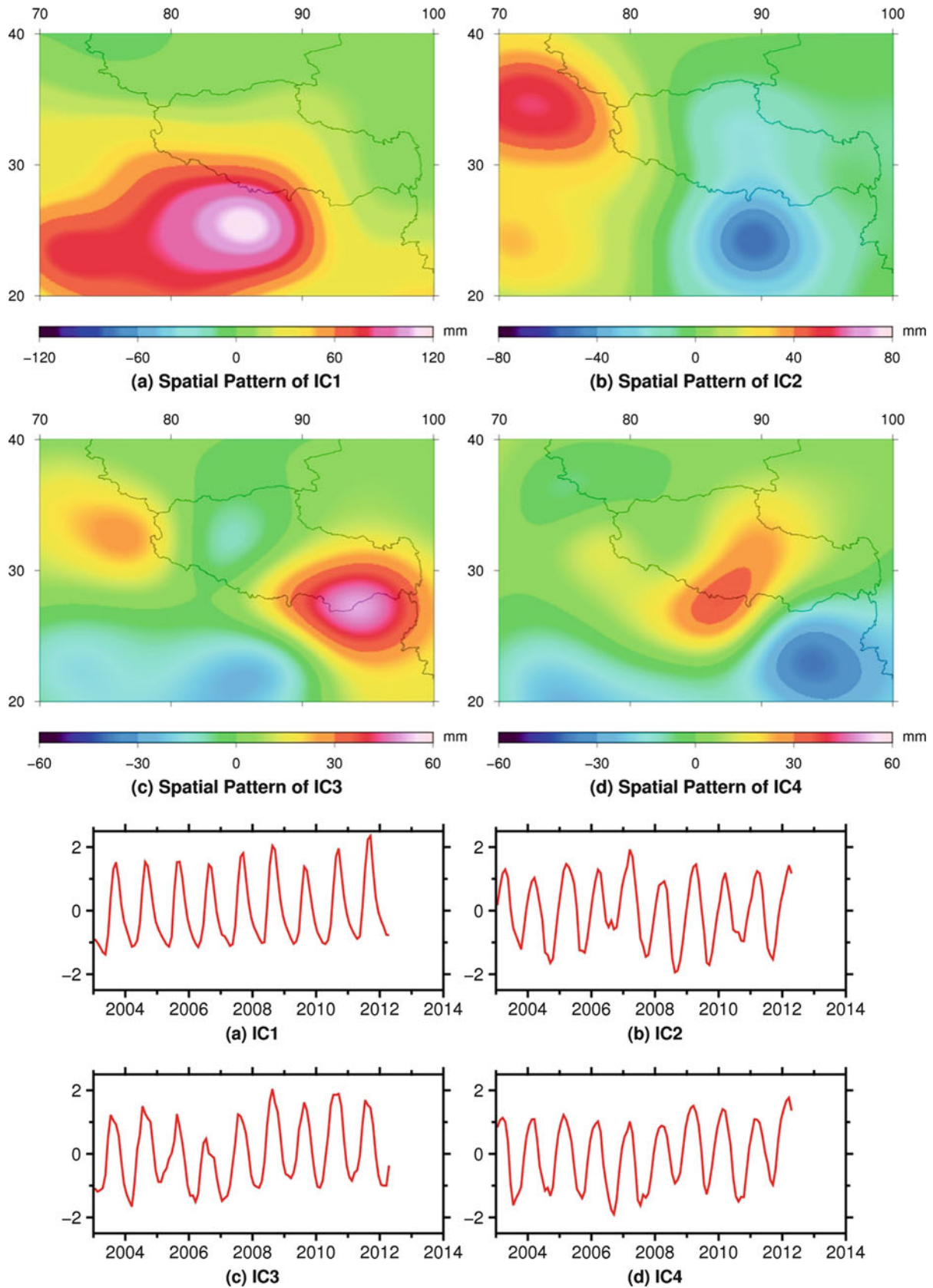


Fig. 5 Spatial pattern (*up*) and time series (*down*) by ICA analysis using 112 months WGHM

Fig. 6 Comparison of time series results of GRACE and hydrological models by ICA analysis

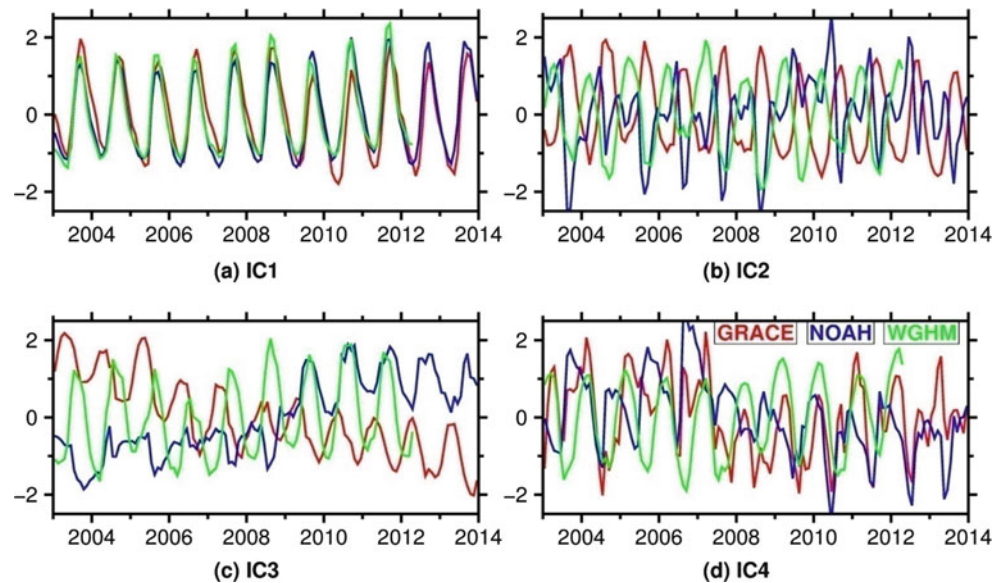


Table 1 Correlation coefficients of GRACE&NOAH and GRACE&WGHM

Coefficients	IC1	IC2	IC3	IC4
GRACE&NOAH	0.884	-0.500	-0.662	0.404
GRACE&WGHM	0.877	-0.874	0.256	0.454

of IC1 from Table 1 is relevant strongly. From spatial patterns, the amplitudes of GRACE-derived water storage changes are larger than that of hydrological models, because the GRACE-derived water storage changes also may include groundwater changes. We can see that the water storage of the Tibetan Plateau in the southwest region has been reduced in recent years, which is likely due to the glaciers melting and snowpack shrinking caused by climate warming (Xu and Zhang 2013). With the analysis of temporal and spatial variation of water reserves, we could further study the impact of natural and anthropogenic factors on the regional climate.

ICA is able to separate independent signal components from data with a little priori information, which has a good prospect in information extraction of GRACE gravity observations and hydrological models. However, some problems still need to be solved in practical applications. How to utilize ICA method to analyze data more effectively, as well as the applicability of the method still need further study.

Acknowledgements The authors are grateful to Ehsan Foroootan and two anonymous reviewers for their constructive comments which led to the improvement of the manuscript. The research is funded by National Key Basic Research Program (2013CB733302), National Natural Science Foundation of China (41274031, 41404014), Chinese Academy of Surveying and Mapping Fundamental Scientific Research Expenses (7771415).

References

- Bartlett MS (2001) Face image analysis by unsupervised learning. Kluwer, Boston. doi:[10.1007/978-1-4615-1637-8](https://doi.org/10.1007/978-1-4615-1637-8)
- Boergens E, Rangelova E, Sideris MG, Kusche J (2014) Assessment of the capabilities of the temporal and spatiotemporal ICA method for geophysical signal separation in GRACE data. *J Geophys Res Solid Earth* 119(5):4429–4447
- Cardoso JF (1992) Fourth-order cumulant structure forcing: application to blind array processing. In: *Statistical signal and array processing, 1992 conference proceedings, IEEE Sixth SP Workshop on IEEE*, pp 136–139. doi:[10.1109/SSAP.1992.246830](https://doi.org/10.1109/SSAP.1992.246830)
- Cardoso JF (1999) High-order contrasts for independent component analysis. *Neural Comput* 11(1):157–192. doi:[10.1162/089976699300016863](https://doi.org/10.1162/089976699300016863)
- Cardoso JF, Souloumiac A (1993) Blind beamforming for non-Gaussian signals. In: *IEEE Proceedings F (Radar Signal Proc)* 140(6):362–370. IET Digital Library. doi:[10.1049/ip-f-2.1993.0054](https://doi.org/10.1049/ip-f-2.1993.0054)
- Chen JL, Rodell M, Wilson CR, Famiglietti JS (2005) Low degree spherical harmonic influences on Gravity Recovery and Climate Experiment (GRACE) water storage estimates. *Geophys Res Lett* 32(14). doi:[10.1029/2005GL022964](https://doi.org/10.1029/2005GL022964)
- Chen JL, Wilson CR, Blankenship DD, Tapley BD (2006) Antarctic mass rates from GRACE. *Geophys Res Lett* 33(11). doi:[10.1029/2006GL026369](https://doi.org/10.1029/2006GL026369)
- Döll, P, Kaspar, F, Lehner, B (2003) A global hydrological model for deriving water availability indicators: model tuning and validation. *Journal of Hydrology*, 270(1):105–134.
- Duan XJ, Guo JY, Shum CK, Van Der Wal W (2009) On the post-processing removal of correlated errors in GRACE temporal gravity field solutions. *J Geod* 83(11):1095–1106
- Forootan E, Kusche J (2012) Separation of global time-variable gravity signals into maximally independent components. *J Geod* 86(7):477–497. doi:[10.1007/s00190-011-0532-5](https://doi.org/10.1007/s00190-011-0532-5)
- Forootan E, Kusche J (2013) Separation of deterministic signals, using independent component analysis (ICA). *Stud Geophys Geod* 57:17–26. doi:[10.1007/s11200-012-0718-1](https://doi.org/10.1007/s11200-012-0718-1)

- Forootan E, Rietbroek R, Kusche J, Sharifi MA, Awange JL, Schmidt M, Famiglietti J (2014) Separation of large scale water storage patterns over Iran using GRACE, altimetry and hydrological data. *Remote Sens Environ* 140:580–595. doi:[10.1016/j.rse.2013.09.025](https://doi.org/10.1016/j.rse.2013.09.025)
- Frappart F, Ramillien G, Maisongrande P, Bonnet MP (2010) Denoising satellite gravity signals by independent component analysis. *Geosci Remote Sens Lett IEEE* 7(3):421–425. doi:[10.1109/LGRS.2009.2037837](https://doi.org/10.1109/LGRS.2009.2037837)
- Guo J, Mu D, Liu X, Yan H, Dai H (2014) Equivalent water height extracted from GRACE gravity field model with robust independent component analysis. *Acta Geophys* 62(4):953–972. doi:[10.2478/s11600-014-0210-0](https://doi.org/10.2478/s11600-014-0210-0)
- Hyvarinen A (1999) Survey on independent component analysis. *Neur Comput Surv* 2(4):94–128
- Hyvärinen A, Karhunen J, Oja E (2004) *Independent component analysis*, vol 46. Wiley, New York
- Jeffers JNR (1967) Two case studies in the application of principal component analysis. *Appl Stat* 225–236
- Jolliffe IT (2003) A cautionary note on artificial examples of EOFs. *J Clim* 16(7):1084–1086. doi:[10.1175/1520-0442\(2003\)016<1084:ACNOAE>2.0.CO;2](https://doi.org/10.1175/1520-0442(2003)016<1084:ACNOAE>2.0.CO;2)
- Luo F, Dai W, Tang C, Huang D, Wu X (2012) EMD-ICA with reference signal method and its application in GPS multipath. *Acta Geod Cartogr Sin* 41(3):366–371
- Lv W, Chen Y, Zhang B (2007) Application of independent component analysis method in earthquake signal de-noise. *Oil Geophys Prospect* 42(2):132–136
- Makeig S, Bell AJ, Jung TP, Sejnowski TJ (1996) Independent component analysis of electroencephalographic data. *Adv Neur Inform Proc Syst* 145–151
- Niu T, Chen LX, Wang W (2002) REOF analysis of climatic characteristics of winter temperature and humidity on Xizang-Qinghai Plateau. *J Appl Meteorol Sci* 135:560–570
- Price AL, Patterson NJ, Plenge RM, Weinblatt ME, Shadick NA, Reich D (2006) Principal components analysis corrects for stratification in genome-wide association studies. *Nat Genet* 38(8):904–909. doi:[10.1038/ng1847](https://doi.org/10.1038/ng1847)
- Rangelova E, van der Wal W, Braun A, Sideris MG, Wu P (2007) Analysis of gravity recovery and climate experiment time-variable mass redistribution signals over North America by means of principal component analysis. *J Geophys Res* 112(F3). doi:[10.1029/2006JF000615](https://doi.org/10.1029/2006JF000615)
- Rodell M, Houser PR, Jambor UEA, Gottschalck J, Mitchell K, Meng CJ, Toll D (2004) The global land data assimilation system. *Bull Am Meteorol Soc* 85(3):381–394. doi:[10.1175/BAMS-85-3-381](https://doi.org/10.1175/BAMS-85-3-381)
- Schmidt R, Petrovic S, Güntner A, Barthelmes F, Wunsch J, Kusche J (2008) Periodic components of water storage changes from GRACE and global hydrology models. *J Geophys Res Solid Earth* 113(B8). doi:[10.1029/2007JB005363](https://doi.org/10.1029/2007JB005363)
- Schrama EJO, Wouters B, Lavallo DA (2007) Signal and noise in Gravity Recovery and Climate Experiment (GRACE) observed surface mass variations. *J Geophys Res* 112, B08407. doi:[10.1029/2006JB004882](https://doi.org/10.1029/2006JB004882)
- Tapley BD, Bettadpur S, Watkins M, Reigber C (2004) The gravity recovery and climate experiment: mission overview and early results. *Geophys Res Lett* 31(9). doi:[10.1029/2004GL019920](https://doi.org/10.1029/2004GL019920)
- Wen H, Zhu G, Cheng P, Chang X, Liu H (2011) The ice sheet height changes and mass variations in Antarctica by using ICESat and GRACE data. *Int J Image Data Fusion* 2(3):255–265. doi:[10.1080/19479832.2010.491803](https://doi.org/10.1080/19479832.2010.491803)
- Werth S, Güntner A (2010) Calibration analysis for water storage variability of the global hydrological model WGHM. *Hydrol Earth Syst Sci* 14(1):59–78. doi:[10.5194/hessd-6-4813-2009](https://doi.org/10.5194/hessd-6-4813-2009)
- Xu P, Zhang W (2013) Inversion of terrestrial water storage changes in recent years for Qinghai-Tibetan plateau and Yarlung Zangbo River basin by GRACE. *J Water Resour Water Eng* 1:007
- Zhang G, Yao T, Xie H, Kang S, Lei Y (2013) Increased mass over the Tibetan Plateau: from lakes or glaciers? *Geophys Res Lett* 40(10):2125–2130
- Zhu G, Li J, Wen H, Wang J (2008) Study on variations of global continental water storage with grace gravity field models. *J Geod Geodyn* 28(5):39–44
- Zotov L, Shum C (2010) Multichannel singular spectrum analysis of the gravity field data from GRACE satellites. In: Chakrabarti SK, Zhuk AI, Bisnovaty-Kogan GS (eds) *Astrophysics and cosmology after Gamow*, vol 1206. Am Inst Phys, Odessa, Ukraine, pp 473–479. doi:[10.1063/1.3292557](https://doi.org/10.1063/1.3292557)